Pergamon

Tetrahedron 57 (2001) 7431–7448

TETRAHEDRON

Tetrahedron report number 581

β-Turn mimetic library synthesis: scaffolds and applications

Andrew J. Souers and Jonathan A. Ellman*

Department of Chemistry, Center for New Directions in Organic Synthesis, University of California, Berkeley, CA 94720, USA†

Received 12 April 2001

Contents

1. Introduction

The poor receptor subtype selectivity, poor biostability and unfavorable absorption properties that often accompany therapeutically relevant peptides has generated a considerable amount of interest in the design of high affinity and selective peptidomimetics.[1] This is usually accomplished by the systematic replacement of backbone amide bonds or the incorporation of constrained elements. In a successfully designed peptidomimetic, the essential amino acid side chains of the corresponding peptide are displayed on an alternative scaffold such that the spatial orientation of the side chains corresponds to the display in the bioactive conformation of the peptide.[2]

β-Turns, **1**, are one of the three major secondary structural elements of peptides and proteins and play a key role in many of the molecular recognition events in biological systems[3] (Fig. 1). These events include but are not limited to the interactions between peptide hormones and their receptors, antibodies and antigens, and regulatory enzymes and their corresponding substrates. A great deal of effort has therefore focused on the design and synthesis of small constrained mimetics of turn structure to provide a better understanding of the molecular basis of peptide and protein interactions in addition to providing potent and selective therapeutic agents.[4] A majority of these efforts, however, have met with only limited success due to difficulties in identifying the key turn residues and the relative orientations of those residues in the receptor bound conformation.[5] This is compounded by the fact that efficient methods for

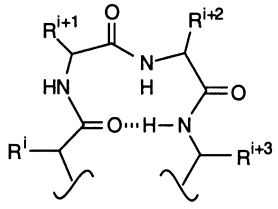

1

Figure 1. β-Turn motif.

* Corresponding author. Tel.: +510-642-4488; fax: +510-642-8369; e-mail: jellman@uclink.berkeley.edu; ellman@collchem.cchem.berkeley.edu

† The Center for New Directions in Organic Synthesis is supported by Bristol–Myers Squibb as Sponsoring Member.

PII: S0040-4020(01)00680-9

constructing turn mimetics incorporating the amino acid side chains corresponding to the i through the $i+3$ positions of these motifs have only recently been developed. Finally, while the retention or improvement of biological activity is the ultimate indicator of successful design, the success of many efforts has been measured by the ability of a scaffold to adopt a turn motif using spectroscopic methods such as circular dichroism or solution phase NMR.

The aforementioned difficulties in identifying the optimal structure for a given turn mimetic could be overcome by the synthesis and screening of libraries of β-turn mimetics that include many possible side chain combinations as well as multiple relative orientations of the side chains. Over the past five years, considerable progress has been made towards this end by both academic and industrial researchers. Multiple reports of parallel synthesis methodologies for turn mimetic synthesis have been disclosed, several libraries have been produced, and biologically active turn mimetics have been identified to several different targets.

The objective of this review is to provide a synopsis of the current state of the art of combinatorial turn mimetic synthesis and scaffold design, in addition to the applications of these technologies to biological targets. The examples are confined to small molecule turn scaffolds that have been designed with diversity and parallel execution in mind, thus, turn-inducing peptide isosteres[6] and cyclic peptides[7] will not be included.

2. β-Turn mimetic classification

Turn mimetics can be categorized into two distinct groups; internal and external.[5] Internal mimetics are constructed upon skeletons that lie within the pseudo 10-membered ring framework of the turn motif, and place an emphasis on side chain presentation as displayed by the pioneering structures of Kahn[4a] **2** and Olson[8] **3** (Fig. 2).

The external mimetics are often constructed on dipeptide isostere skeletons that do not display side chain functionality at the central $i+1$ and $i+2$ positions. These structures reduce the conformational flexibility of a peptide with a rigidified skeleton that lies outside of the turn's general framework, and are primarily employed to orient the surrounding peptide chain into a turn conformation. Structures **4**[9] and **5**[10] developed by Freidinger and Nagai, respectively, are notable examples (Fig. 3).

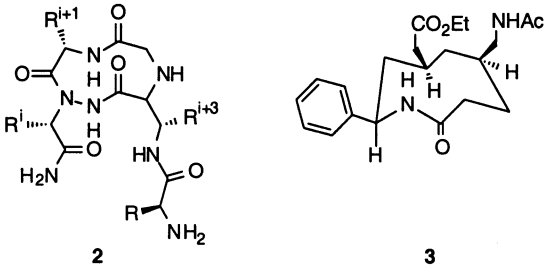

Figure 2. Internal turn mimetics.

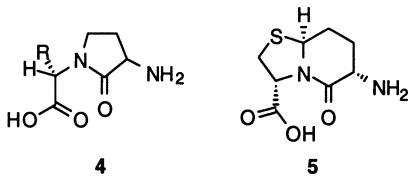

Figure 3. External turn mimetics.

3. Medium ring heterocycles

3.1. First generation mimetics and applications

Virgilio and Ellman developed the first method for the solid-phase synthesis of libraries of β-turn mimetics.[11] The medium ring heterocyclic turn mimetic **6** is constructed from three readily available components, with the $i+1$ and $i+2$ side chains being derived from an α-halo acid and an α-amino acid, respectively. The mimetic is constrained in a turn structure by replacing the hydrogen bond between the i and $i+3$ residue with a covalent thioether backbone linkage (Fig. 4). Both the flexibility of the turn mimetic as well as the relative orientations of the side chains can be varied by introducing different backbone linkages to provide medium to large sized rings. In addition, different side chain orientations are obtained by introducing different absolute configurations at each of the stereocenters introduced by the $i+1$ and $i+2$ side chains of the turn mimetic.

In the initial studies, the β-turn mimetics were synthesized using PEG-PS with a Rink amide linker. Prior to backbone functionalization, a *p*-nitrophenylalanine residue was loaded onto the support to serve as a convenient UV tag for accurate determination of the overall purity of the turn mimetic by HPLC (vide infra). α-Bromoacetic acid was first coupled to the support-bound *p*-nitrophenylalanine to afford **7** (Scheme 1). Subsequent treatment with the aminoalkyl thiol protected as the *t*-butyl mixed disulfide provided the support-bound amine **8**. The secondary amine was then coupled with the desired *N*-Fmoc-α-amino acid followed by treatment with 20% piperidine in DMF to afford the immobilized amino amide **9**. Addition of the symmetric anhydride of the appropriate α-bromo acid[12] then provided the acyclic intermediate **10**. Cleavage of the mixed disulfide was then accomplished by treatment of the cyclization precursor with tributylphosphine in a 5:3:2 propanol/DMF/H_2O comixture. Finally, cyclization to provide the nine- or 10-membered thioether was accomplished by treatment with tetramethylguanidine (TMG) in a DMF/H_2O comixture, and cleavage of the turn mimetic **11** from the support occurred upon treatment with 95:5:5 TFA/Me_2S/H_2O.

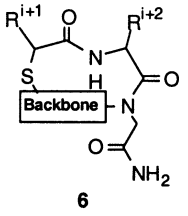

Figure 4. Medium ring heterocyclic scaffold.

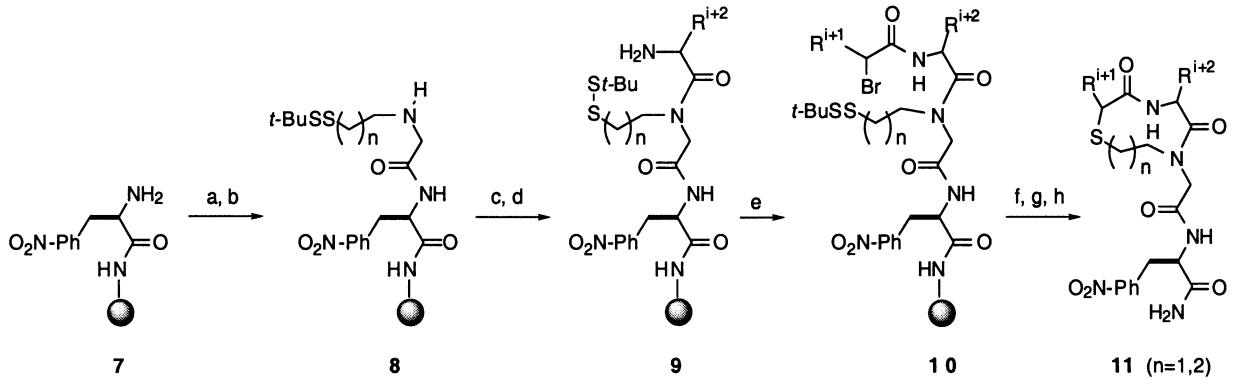

Scheme 1. (a) α-Bromoacetic acid, 1,3-diisopropylcarbodiimide; (b) 2-Aminoethanethiol-*t*-butyl disulfide or 3-aminopropanethiol-*t*-butyl disulfide; (c) *N*-Fmoc-α-amino acid, *O*-(7-azabenzotriazol-1-yl)-*N*,*N*,*N*′,*N*′-tetramethyluronium hexafluorophosphate; (d) 20% piperidine in DMF; (e) symmetric anhydride of α-bromo acid; (f) tributylphosphine, H_2O; (g) *N*,*N*,*N*′,*N*′-tetramethylguanidine; (h) 1:1:18 H_2O/Me_2S/trifluoroacetic acid.

Employing this synthesis sequence, 11 turn mimetics were obtained with an average purity of 75% over the eight-step process as determined by HPLC analysis (Table 1). Any side-products that were produced during the synthesis of the turn mimetic would be detected by HPLC analysis since the UV tag (*p*-nitrophenylalanine) was introduced before the synthesis of the mimetic was initiated. For all of the turn mimetics synthesized, cyclization provided the desired cyclic monomer with no cyclic dimer detected (<5%). This includes mimetics incorporating both (*R*) and (*S*) α-bromo acids and sterically hindered components such as α-bromoisovaleric acid. A variety of side chain functionality could be incorporated successfully into the turn mimetics including alcohol, phenol, carboxylic acid and amine functionality. In addition, minimal racemization was observed in the synthesis sequence (<5% by HPLC).

To demonstrate the utility of the synthesis sequence for the rapid construction of turn mimetics libraries, the 11 mimetics were resynthesized simultaneously employing the Chiron Mimotopes pin apparatus.[13] All 11 derivatives were obtained in a very high level of purity as determined by HPLC analysis (Table 1). Based on these results, a library of 1,152 β-turn mimetics was prepared using 19 α-bromo acids, 34 α-amino acids, and two backbone elements to provide the nine- and 10-membered cyclic mimetics, respectively. To reduce the number of pins handled while keeping the work required for deconvolution to a minimum, the two aminoalkyl backbone components were introduced into each well as an equimolar mixture. After completion, the library was characterized by electrospray mass spectroscopy, with 30 wells (7%) being selected at random. Of the wells tested, 29 of 30 showed the correct mass ions, with the lone unsuccessful entry containing an *N*-methylglycine.

Table 1. β-Turn mimetics **11** (Scheme 1)

Entry	R^{i+1}	R^{i+2}	*n*	Purity (%)[a] PEG-PS	Pins
1	CH_3	$CH_2C_6H_5$	2	90	79
2	CH_3[b]	$CH_2C_6H_5$	2	59	90
3	$CH(CH_3)_2$	$CH_2C_6H_5$	2	81	86
4	CH_3CO_2H	$CH_2C_6H_5$	2	65	79
5	CH_3	$(CH_2)_4NH_2$	2	72	87
6	CH_3	CH_2CO_2H	2	63	86
7	H	$CH_2C_6H_5$	2	85	91
8	H	CH_2OH	2	82	93
9	CH_3	$CH_2C_6H_4$-4-OH	2	74	88
10	CH_3	$CH_2C_6H_5$	1	77	75
11	$CH_2C_6H_4$-4-OH	CH_3	1	81	90

The stereochemical configuration at the $i+1$ site is *R* and at the $i+2$ site is *S* unless otherwise specified.
[a] Purity by HPLC.
[b] The stereocenter has the *S* configuration.

3.2. Second generation mimetics and optimization efforts

Virgilio and Ellman reported the synthesis of a second

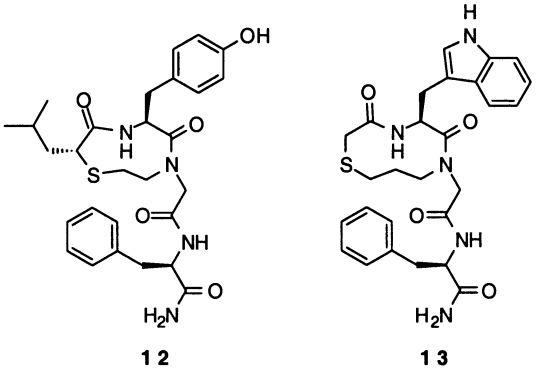

Figure 5. Active ligands to the fMLF receptor.

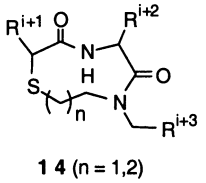

Figure 6. Second generation medium ring scaffold.

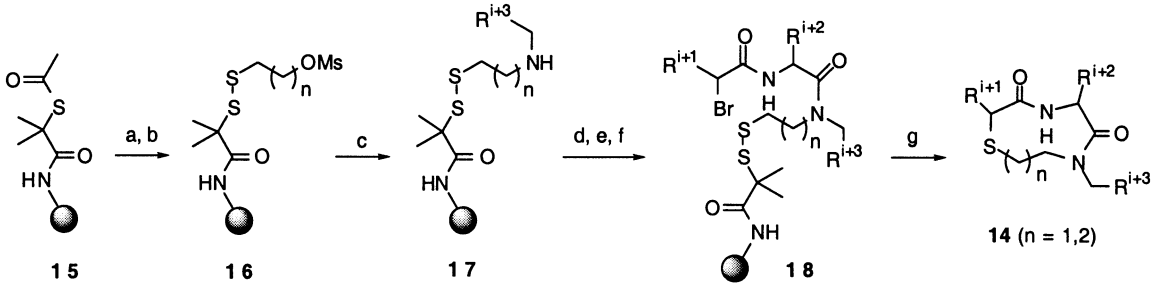

Scheme 2. (a) NaOMe, 3:1 THF/MeOH; (b) *S*-thiobenzothiazole-β-hydroxy-ethyl disulfide, THF; (c) primary amine, NMP, 50°C; (d) *N*-Fmoc-α-amino acid, *O*-(7-azabenzotriazol-1-yl)-*N*,*N*,*N*′,*N*′-tetramethyluronium hexafluorophosphate, *i*-Pr_2NEt, DMF; (e) 20% piperidine, DMF; (f) α-Bromo acid, 1,3-diisopropylcarbodiimide, DMF; (g) $(HO_2CCH_2CH_2)_3P$, 9:1 dioxane/H_2O, PS-TMG.

generation of β-turn mimetics **14** which were designed to possess improved binding affinity, solubility, and perhaps bioavailability by eliminating the primary amide functionality while simultaneously presenting a third point of contact in the form of the $i+3$ residue (Fig. 6).[15] The synthesis of this later generation turn mimetic involves two major modifications (Scheme 2). First, side chain functionality at the $i+3$ position is introduced by means of a primary amine. Second, attachment to the solid support during the solid-phase synthesis sequence is accomplished by using a disulfide linkage rather than the Rink amide linkage that was employed in the synthesis of mimetic **11**. When the final cyclic product **14** is formed, no vestiges of the linkage to the support remain.

The second generation turn mimetic is amenable to the rapid and simultaneous synthesis of a number of derivatives. Mimetic **14** is assembled from four components in eight steps on a solid support. An α-halo acid supplies the $i+1$ side chain, a Fmoc-protected α-amino acid supplies the $i+2$ side chain, a primary amine furnishes the $i+3$ side chain, and a hydroxyalkyl thiol provides the backbone component (Scheme 2).

Solid-phase synthesis was initiated by methanolysis of support-bound linker **15** followed by disulfide interchange with a mixed disulfide to afford the support-bound mesylate **16**. This intermediate was then treated with a concentrated solution of the appropriate primary amine in NMP to introduce the $i+3$ side chain of **17**. The $i+2$ and $i+1$ side chains were then incorporated by coupling an Fmoc-α-amino acid followed by Fmoc deprotection, and then coupling of an α-bromo acid to afford the linear support-bound precursor **18**. The acyclic turn mimetic was then cleaved from the resin with tris-carboxyethyl phosphine and treated with support-bound guanidine. The latter reagent serves to remove all phosphine and phosphine oxide byproducts, as well as HBr, in addition to catalyzing the cyclization. Filtration and concentration consistently afforded the cyclized mimetics **14** in good yields over eight steps on support from the aminomethylated polystyrene (59% average overall yields), with very small amounts (<5%) of the minor $i+1$ epimer being the only significant byproduct (Table 2).

In order to first establish the ability of heterocycle **14** to serve as a highly effective mimetic of peptide and protein structure, the authors explored the development of potent ligands to the somatostatin receptors.[16] A focused library of somatostatin mimetics (Fig. 7) was designed based upon prior extensive studies of analogs of this peptide.[17] Seminal work by Veber demonstrated that D-Trp in the eighth residue of somatotropin release inhibiting factor (SRIF) lead to increased levels of potency and stability.[18] In a different study, Goodman and co-workers identified an active retro-enantio analog of somatostatin wherein both the order and stereochemistry of the central Trp and Lys residues are reversed.[19] These examples indicated that several alternative displays of the tryptophan and lysine side chains could potentially provide active compounds. For this reason all eight possible stereochemical and positional combinations of the Trp and Lys side chains were included at the $i+1$ and $i+2$ positions. Twenty-two different amines were introduced at the $i+3$ position. Of these, eight hydrophobic amines were chosen for their similarity to the $i+3$ (Phe and Tyr) as well as the i (Thr and Val) residues present in numerous somatostatin analogs. The remaining 14 amines

Table 2. Synthesis of β-turn mimetics **14**

Entry	R^{i+1}	R^{i+2}	R^{i+3}	n	Yield (%)[a]	Purity (%)[b]
1	CH_3	CH_3	CH_2SPh	1	60	92
2	CH_3	$CH_2CH(CH_3)_2$	CH_2SPh	1	64	94
3	CH_3	$(CH_2)_4NHBoc$	$CH(CH_3)_2$	1	56	86
4	H	$CH_2C(O)OtBu$	$CH_2CH(CH_3)_2$	1	59	93
5	$CH_2CH(CH_3)_2$	CH_2C_6H-4-O*t*Bu	CH_2Ph	2	34	85
6	$CH(CH_3)_2$	CH_3	2,4,6-(MeO)Ph	2	51	94
7	CH_2(Boc)In	$(CH_2)_4NHBoc$	$CH_2CH(Ph)_2$	1	59	84
8	CH_2(Boc)In	$(CH_2)_4NHBoc$ (*R*)	c-Propyl	1	59	93

The stereochemical configuration of the α-carbon at the $i+1$ site is *R* and at the $i+2$ site is *S* unless otherwise specified.

[a] Mass balance yields of purified, analytically pure material are based upon the approximate loading level of **15**.

[b] The purity of the crude product directly off of the support is determined by reverse phase HPLC, 60–100% CH_3OH in 0.1% aqueous TFA as monitored at 220, 254, or 280 nM.

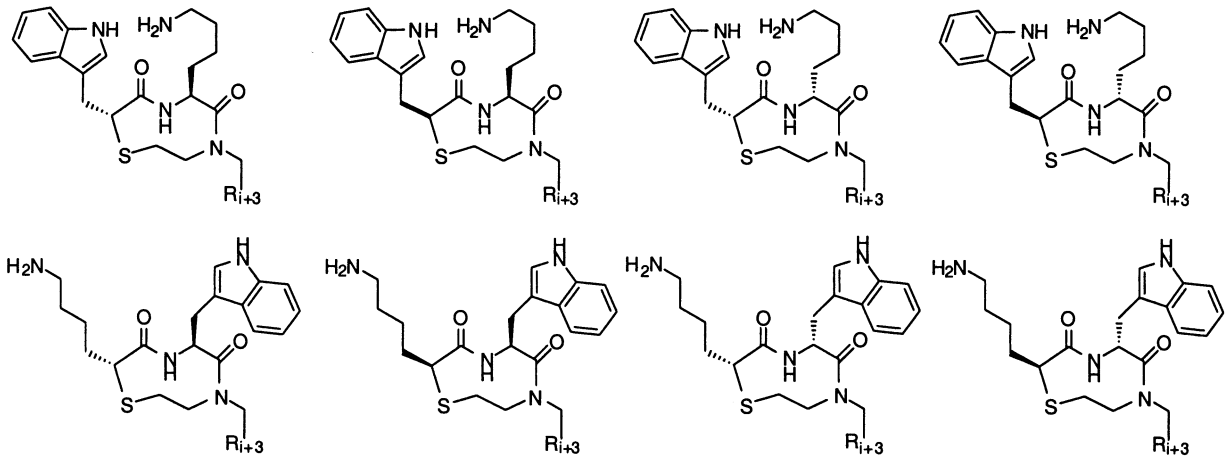

Figure 7. Focused library of somatostatin mimetics.

Table 3. IC_{50} values (μM) for the most potent scaled-up somatostatin mimetics (values reflect assay results of purified material)

Ligand	hsst1	hsst2	hsst3	hsst4	hsst5
19	1.10	0.158	1.18	0.479	0.589
20	0.851	0.252	0.135	0.245	0.120
21	0.501	1.59	3.09	1.05	0.0870
22	2.24	3.63	0.813	0.363	0.832
23	4.47	4.57	1.20	3.16	1.20

were selected to maximize the diversity of functionality at this site employing a hierarchical, 2D structure key-based clustering algorithm developed by MDL information systems.[20]

The compounds were individually screened against all five cloned human somatostatin receptor sub-types (hsst1–5). The turn mimetics were tested for inhibition of binding of ({^{125}I}-{Tyr11}-SRIF) to recombinant hsst1, hsst3, hsst4 and hsst5 and the binding of ([^{125}I]-BIM-23027) to the recombinant hsst2 all expressed in CHO-K1 cells. The three most active compounds to hsst2, hsst3, and hsst5 (**19**, **20**, **21**, respectively) were prepared on a larger scale for accurate IC_{50} determination on purified and characterized material. In addition, the two stereoisomers **22** and **23** of the most active compound **21** were resynthesized in order to further assess the effect of stereochemistry upon binding. As shown in Table 3, compounds **19** and **21** are potent ligands to subtypes 2 and 5, respectively. In addition, they demonstrate modest to good selectivity over the remaining subtypes.[21] Interestingly, an unanticipated preference for D-Lys was observed at the $i+2$ position, which demonstrates the critical importance of evaluating collections of mimetics (Fig. 8).

Follow up studies on compound **21** were performed with the ultimate goal of improving the potency and subtype selectivity of this lead structure. This was initiated by first assessing the importance of the three side chains in **21** for the observed receptor binding. To this end, three derivatives were prepared with each derivative having one of the three side chains replaced with a methyl substituent, and the compounds evaluated for receptor affinity. None of the derivatives showed significant binding to hsst5 ($IC_{50}>10$ μM) unambiguously establishing the importance of each side chain for binding.

With this SAR data in hand, several methods were explored for rigidifying the backbone of compound **21** in order to identify the ideal active geometry of the mimetic. Specifically, the lysine residue in the lead structure presented the opportunity for the incorporation of constrained amino acids. Since both proline and pipecolic acid could be used effectively in the solid-phase synthesis sequence, constrained lysine analogs of these amino acids were selected. Because ligand **21** possesses the unnatural D stereochemistry at the $i+2$ position, five-membered ring lysine analogs which retain this stereochemistry at the α-carbon were designed. These amino acids differed in the stereochemistry at the four-position in order to probe the orientational preference of the side chain while locking the heterocyclic backbone. A six-membered ring lysine derivative was also designed to retain the unnatural D stereochemistry at the α-carbon, while the side chain is oriented in

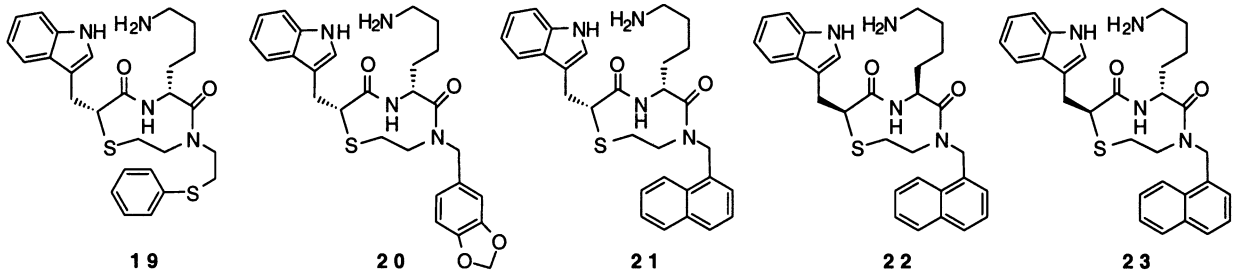

Figure 8. Scaled-up somatostatin ligands.

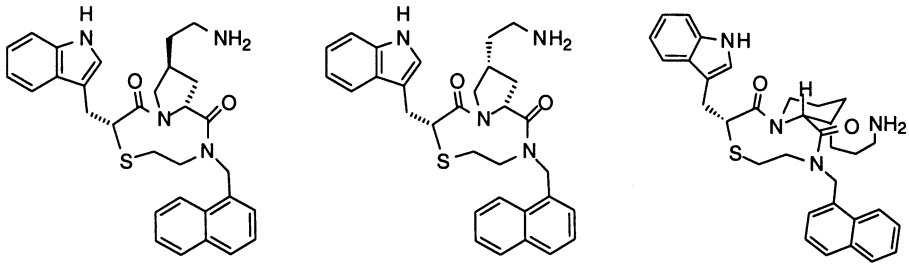

24 **25** **26**

Figure 9. Second-generation constrained mimetics.

a manner cis to the carboxylate in order to place the ϵ-amine in close proximity to the tryptophan pharmacophore.[22,23] The three constrained lysine surrogates were synthesized according to literature methods with only minor modifications,[22] and then incorporated via solid-phase synthesis into the protected turn mimetics **24**–**26** as described previously (Fig. 9).

The three individual mimetics were then tested at a concentration of 1 μM in a competitive radioligand binding assay against ({^{125}I}-{Tyr11}-SRIF) in membranes from CHO-K1 cells expressing human sst1–sst5. Control compound **21** showed complete inhibition of SRIF binding to hsst5 at 1 μM, while compounds **24** and **25** inhibited hsst5 at 50 and 56%, respectively. Bicyclic compound **26** exhibited complete inhibition at hsst4 and hsst5, respectively, while showing modest inhibition for the remaining subtypes.

A full IC_{50} curve was performed on the active mimetic **26**. As depicted in Table 4, the inhibitory constants for hsst4 and hsst5 are both 41 nM. The dual activity and selectivity for these subtypes over the other receptor subtypes is quite interesting given that these two receptors come from distinct groups. Furthermore, the IC_{50} value of 41 nM is a two-fold enhancement over compound **21** for hsst5, but over 25-fold for hsst4. Thus, while the constrained six-membered amino acid clearly imparts enhanced potency on mimetic **26** for the two subtypes, it has the effect of lowering the selectivity for hsst5 over the non-homologous hsst4 when compared to the parent compound **21**.[23]

A large library of turn mimetics that incorporates nearly all of the proteinogenic amino acid side chains at the $i+1$, $i+2$ and $i+3$ positions was also designed for the identification of peptidomimetic ligands to receptors where relatively little information is available regarding the receptor–peptide ligand interactions (Fig. 10).

To construct the library of 5544 spatially separate mimetics, both stereochemistries of 22 α-bromo acids and 28 Fmoc-α-amino acids were utilized at the $i+1$ and $i+2$ positions, respectively, to provide a highly representative cross-section of proteinogenic side chain functionality at these two sites. Nine primary amines were employed at the $i+3$ position on the basis of diversity and compatibility with the overall sequence, and the spatially addressable format was laid out such that an exhaustive display of all side chain/stereochemistry combinations were present. The library was partially analyzed by MALDI-TOF, NMR, and HPLC. Of the 110 compounds sampled, 95% displayed the correct mass ions by mass spectrometry, and proton NMR and HPLC analysis revealed an average of 1.4±0.4 μmol per well, with the small amount of contaminants being residual water or plasticizer.[24]

Table 4. IC_{50} values of compounds **21** and **26** (μM)

Compound	hsst1	hsst2	hsst3	hsst4	hsst5
21	0.501	1.59	3.09	1.05	0.0870
26	0.407	0.275	1.26	0.0410	0.0410

Subsets of the large diverse library were chosen for evaluation against several different biological targets. In one effort towards the identification of $\alpha_4\beta_1$ integrin receptor antagonists, 2304 compounds were selected based on the LDV sequence that had been implicated as the recognition element for the $\alpha_4\beta_1$ integrin receptors.[25] The library of turn mimetics was evaluated for inhibitory effects on the binding of fluorescently labeled Ramos cells to an immobilized CS-1 peptide. The individual library compounds were assayed at a concentration of 1 μM. Nearly all of the active compounds displayed an aspartic acid $i+1$ side chain, with both D and L stereochemistries being represented. Additionally, nearly all active compounds contained a hydrophobic residue at the $i+2$ site.

To validate these inhibitory effects, the large scale syntheses of four of the most active compounds was performed employing the previously described conditions. The four compounds were evaluated using the mentioned assay conditions, and IC_{50} values were determined. The two most potent compounds **27** and **28**, which differ only in their stereochemistry about the $i+1$ position, displayed IC_{50} values of 5 and 8 μM, respectively. At the time of publication, compounds **27** and **28** represented the most potent non-peptide antagonists reported for the $\alpha_4\beta_1$/CS-1 protein–protein interaction (Fig. 11).[26]

In a second effort targeting the melanocortin receptors, 951 compounds were selected based on their similarity to the FRW sequence on the melanotropin peptides.[27] This sequence has been implicated as the key recognition motif for the binding of these peptides to the corresponding melanocortin receptors. The compounds were individually assayed in a fluorescence based physiological response assay,[28] and several active wells were identified. Two of the most active compounds were resynthesized, purified,

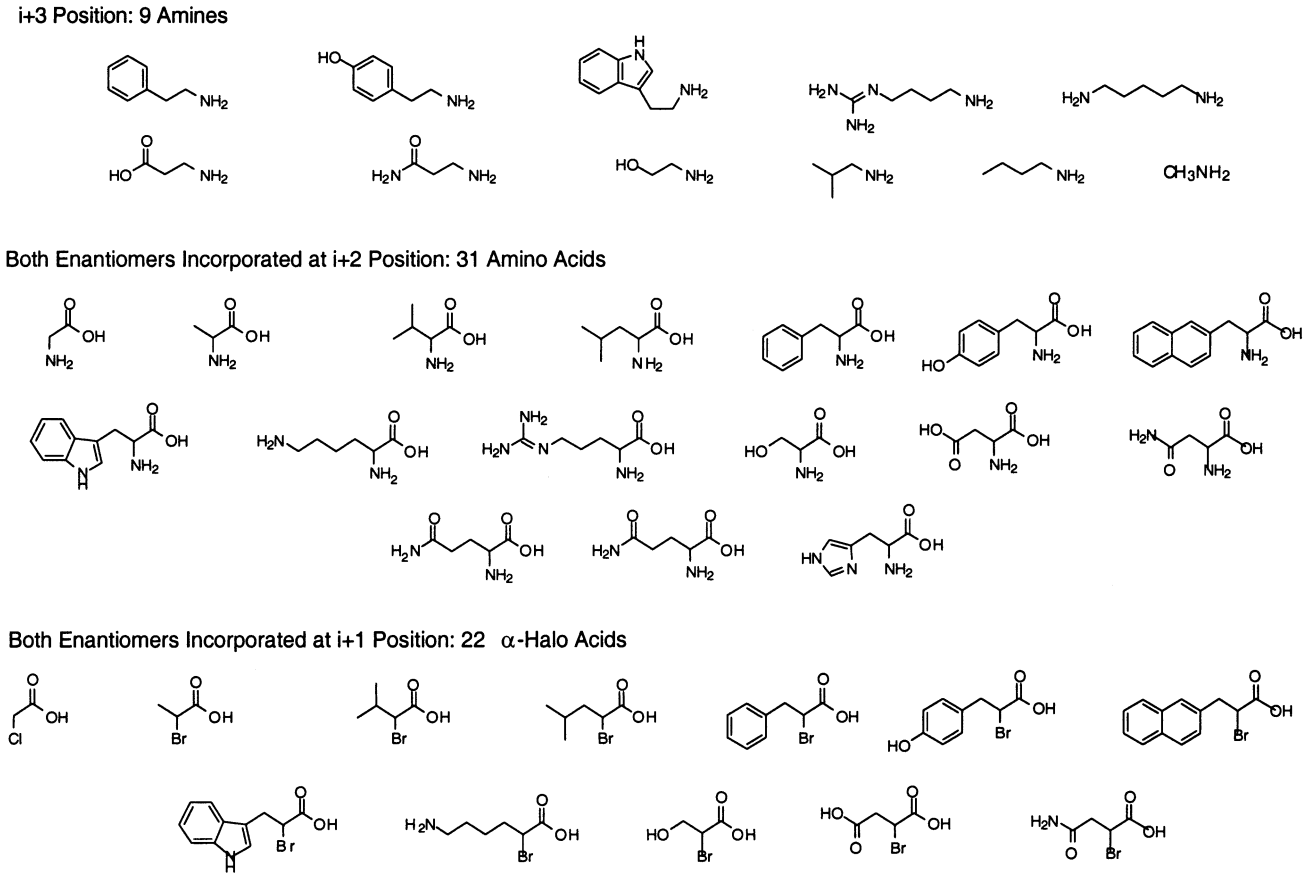

Figure 10. Diverse library components.

characterized, and tested in triplicate in at least two independent experiments at the melanocortin receptor (MCR) subtypes 1, 3, 4, and 5.

Compound **29** (Fig. 12) possesses an EC_{50} of 42.5±6.9 μM at the MC1R, while showing no activity at the MC3R and MC4R, and little agonist activity at the MC5R. Similarly, compound **30** showed an EC_{50} value of 63.4±2.9 μM at MC1R, with no significant agonist activity at the remaining subtypes. At the time of publication, these structures represented the first non-peptide agonists reported for any of the melanocortin receptors.[29]

Finally, Kondo and co-workers reported an application of mimetic **14** for the rigidification of a manosyl Ser-Glu dipeptide that was previously identified as a potent mimetic of sialyl Lewis x.[30] Computational studies indicated that the selectin bound form of linear mimetic **31** adopted a type II or II′ β-turn geometry (Fig. 13). To test this hypothesis, the authors performed the synthesis of sLe^x mimetic **32** based on the 10-membered heterocycle.[20]

The biological activity of sLe^x mimetic **32** was evaluated using an in vitro ELISA assay and the activity compared to sLe^x and linear mimetic **31**. The compound showed weak binding to *E*-selectin relative to **31**, but exhibited potent activity to P- and L-selectin. This study indicated that the heterocyclic skeleton in compound **32** could be a viable scaffold for sLe^x mimetics. The authors reported ongoing studies with alternative ring sizes.

Mimetic **14** has proven to be quite effective for the identification of biologically active compounds. Central to the success of the reported efforts is the capability of preparing

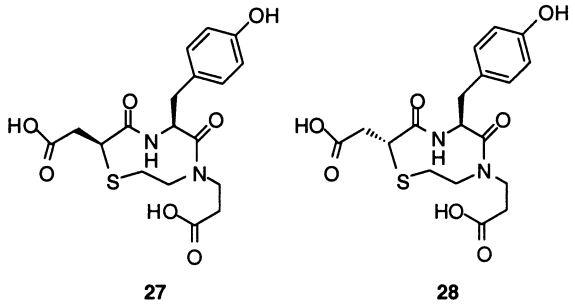

Figure 11. Potent $\alpha_4\beta_1$/CS-1 antagonists.

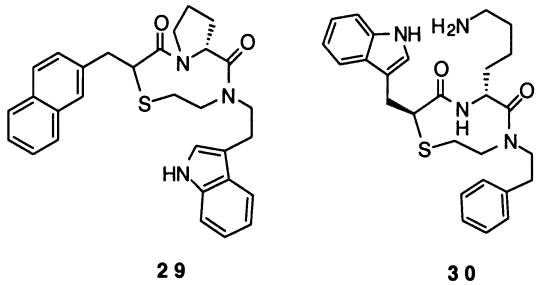

Figure 12. MC1R agonists.

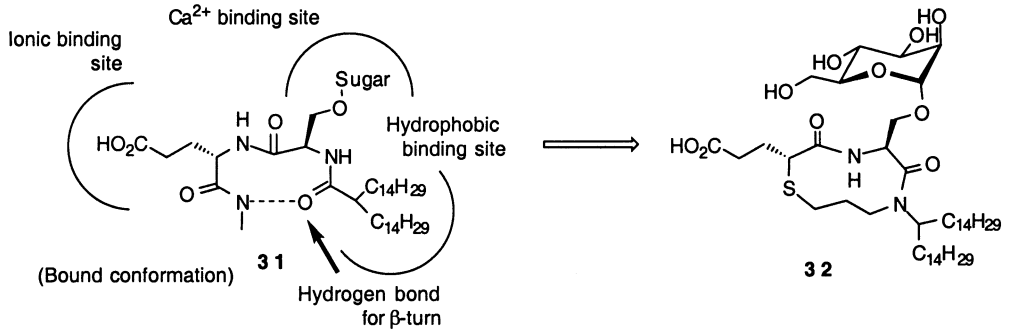

Figure 13. sLe^x Mimetic binding.

heterocycles displaying different side chains corresponding to the $i+1$, $i+2$, and $i+3$ positions of a β-turn, in addition to different side chain stereochemistries. This side chain and orientational diversity can be accessed rapidly with readily available or commercially accessible building blocks, and the ability to synthesize large collections of turn mimetics has been established. Finally, the synthetic sequence accommodates various constrained backbone and side chain elements as demonstrated in the optimization efforts of somatostatin ligand **21**, which culminated in the identification of the more potent second generation compound **26**.

4. Medium ring bicyclic scaffolds

Bicyclic heterocycles, which are non-peptidic in nature, have become a recent focus of β-turn mimetic design and library synthesis. This class currently consists of bicyclic diketopiperazines and tetrahydro-2*H*-pyrazino{1,2-a}pyrimidine-4,7-diones and has the key feature of being accessible by several different synthetic sequences and cyclization strategies. This allows for several possible constructions that utilize different types of building blocks, and indeed, the four examples in this review display four different synthetic routes. Notably, these efforts have culminated in the identification of active turn mimetics to two distinct biological targets.

4.1. Tetrahydro-2*H*-pyrazino{1,2-a}pyrimidine-4,7-diones

Kahn et al. have reported a general strategy for the solid-phase synthesis of bicyclic heterocycle libraries based on a tetrasubstituted tetrahydro-2*H*-pyrazino{1,2-a}pyrimidine-4,7-dione skeleton.[31] Mimetic **33** is constructed from α-amino acids, β-amino acids, acylating agents and sulfonylating agents in seven to nine steps on support. The authors noted that the particular choice of the scaffold was due in large part to the conformational rigidity of the general pyrazino-pyrimidine-dione skeleton (Fig. 14).

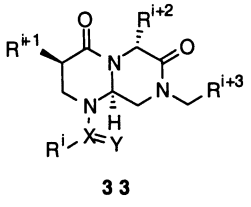

Figure 14. Tetrahydro-2*H*-pyrazino{1,2-a}pyrimidine-4,7-dione scaffold.

The key step in the synthesis is a tandem cleavage and cyclization sequence from a latent aldehyde linker (Scheme 3). The solid-phase generation of the intermediates is carried out by employing two types of support-bound linkers; the acetal linker[32] **A** and the olefin type linker **B**. Diversity was first introduced in the form of the putative $i+3$ position by a primary amine in an S_N2 displacement of the support-bound bromide **34**. The resulting secondary amine **35** was then coupled with an Fmoc-α-amino acid and subsequent piperidine deprotection provided the immobilized amino amide **36**. This intermediate was then coupled with either Fmoc β-amino acids or N^2-Fmoc-N^3-Alloc-2,3-diaminopropionic acid to afford the resin-bound intermediates **37a** or **37b**, respectively. For **37a**, the Fmoc group was removed and the free amine treated with the appropriate aryl or alkyl sulfonyl chloride or alkyl *p*-nitrophenyl carbonate in the presence of *i*-Pr_2NEt to afford intermediate **38**. For **37b**, an additional point of diversity was introduced at the $i+1$ position by removal of the α-amino Fmoc group and subsequent acylation with a carboxylic acid. The β-amino Alloc group was then cleaved with catalytic $Pd(PPh_3)_4$ and $PhSiH_3$, and the resultant amine converted to the corresponding sulfonamide and carbamate products **38**. Cleavage from the acetal linker **A** followed by acylimminium cyclization was performed by treatment with formic acid at room temperature to afford final compounds **40** or **41**. Alternatively, cleavage of the olefin linker **B** was effected by oxidation with a catalytic amount of osmium tetroxide and sodium periodate to liberate a mixture of aldehyde and hemiaminal. After treatment with catalytic TFA in CH_2Cl_2, the cyclization proceeded through the intermediacy of the acylimminum cation to afford the final mimetics (Scheme 3).

Eleven different compounds were synthesized in an average isolated yield of 43% based on the initial loading of the solid support (Table 5). HPLC analysis at 214 nm showed the crude compounds to be the major products in all cases. In addition, 2D NMR demonstrated that a single diastereomer with a trans configuration was formed for the compounds analyzed, although most derivatives of **40** existed as a mixture of two rotamers about the urethane linkage.

To validate the ability of scaffold **33** to produce biologically active turn mimetics, Kahn and co-workers evaluated a collection of 14 compounds for inhibition of binding of the radioligand {^{3}H}DPDPE (D-pen^3, D-pen^5-enkephalin) to the δ and μ opioid receptors. At 10 μM, **42** (Fig. 15) exhibited 60% inhibition and an IC_{50} value of

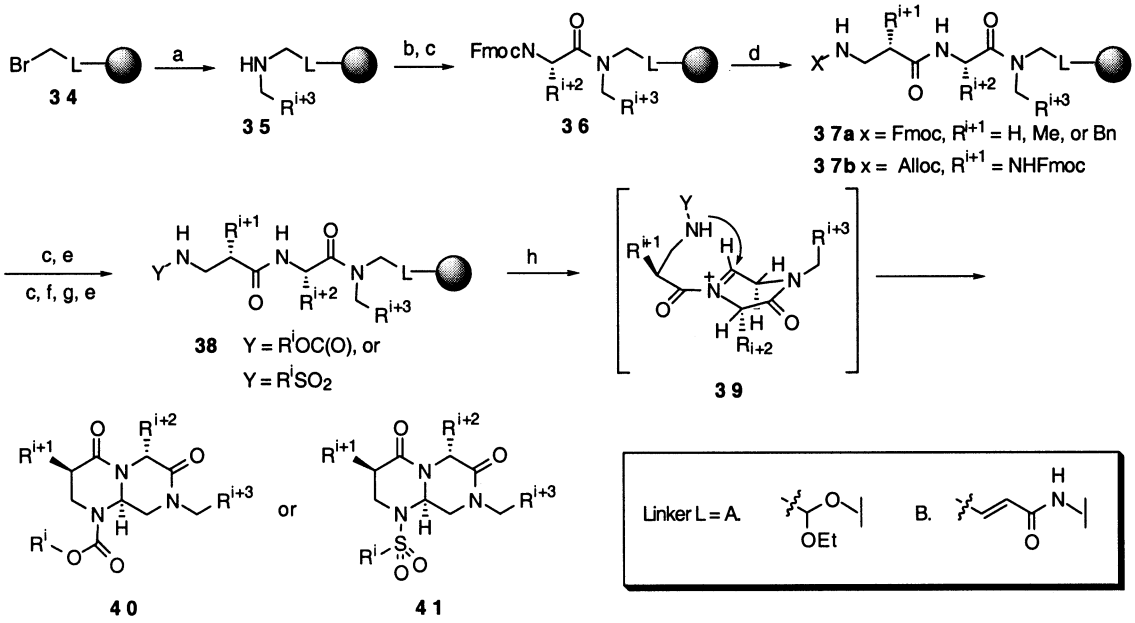

Scheme 3. (a) 2 M primary amine, DMSO; (b) *N*-Fmoc-α-amino acid, 1,3-diisopropylcarbodiimide, 1-hydroxy-7-azabenzotriazole, NMP; (c) 20% piperidine, DMF; (d) *N*-Fmoc-β-amino acid or N^2-Fmoc-N^3-Alloc-2,3-diaminopropionic acid, 1,3-diisopropylcarbodiimide, 1-hydroxy-7-azabenzotriazole; (e) ROC(O)ONp or RSO_2Cl, *i*-Pr_2NEt; (f) RCO_2H, 1,3-diisopropylcarbodiimide, 1-hydroxybenzotriazole; (g) Cat. $Pd(PPh_3)_4$, $PhSiH_3$; (h) Formic acid at rt or cat. $OsO_4/NaIO_4$ then cat. TFA, CH_2Cl_2.

6.9±1.2 μM to the δ opioid receptor. At the same concentration, mimetic **43** was found to inhibit the binding of the radioligand at the 92% level. Mimetic **42** showed a similar 61% inhibition at the μ opioid receptor (IC_{50}= 5.4±0.70 μM), while compound **43** exhibited a 98% inhibition. Compound **42** was also evaluated for in vivo analgesic activity in a mouse tail flick assay, and was found to possess 10–15% of the analgesic activity of morphine (Fig. 15).[33]

In a second application, Kahn and co-workers constructed a library targeting the $\alpha_4\beta_1$ integrin receptor interactions, although the exact number of compounds synthesized and screened was not disclosed. Each compound was individually evaluated for its ability to antagonize the binding of $\alpha_4\beta_1$ expressed on the surface of fluorescently labeled Ramos cells to a linear CS-1 peptide, and active ligands were identified. The authors noted the importance of the carboxylate moiety for binding, and reported the identification of a compound that exhibits an IC_{50} of 0.70 μM towards this protein–protein interaction.[34]

Table 5. Turn mimetics **40** and **41**

Entry	Linker	R^i	R^{i+1}	R^{i+2}	R^{i+3}	Yield[a]
1	A	Bn	H	Bn	*p*-Cl-Ph	71
2	A	Bn	Ac-NH	Me	H	42
3	A	Bn	Bz-NH	Me	H	31
4	A	Bn	Me	Me	H	47
5	A	*p*-OH-PhEt	H	Bn	*n*Bu	36
6	A	Bn	Bn	Bn	*n*Bu	42
7	B	Bn	H	Me	H	33
8	B	Bn	H	*t*BuO_2C-Et	H	22
9	A	Ph	H	Bn	c-Hexyl	57
10	A	Ph	Ac-NH	Me	H	33
11	A	*p*-Tolyl	H	Bn	*p*-Cl-Ph	62

[a] Isolated yield (%) for chromatographically purified compounds based on the initial loading of the solid support (ArgoGelOH or NH_2).

Finally, Kahn and co-workers reported a modification to the existing route that would allow for alternative functionalization of the bicyclic mimetic.[35] Since the diversity at the *i* position was limited to commercially available sulfonyl chlorides or required the preparation of alkyl *p*-nitrophenyl carbonates in solution phase, the authors enhanced the utility of the solid-phase synthesis sequence by employing on-resin urea formation that is amenable to automated synthesis. As shown in Scheme 4, the modified route begins with intermediate **37a**, which was prepared according to the sequence described previously (Scheme 3). To introduce functionality at the *i* position, the Fmoc group was removed with 20% piperidine and subsequently treated with *p*-nitrophenyl chloroformate and *i*-Pr_2NEt in DCM/THF to afford the activated carbamate **44**. Treatment with a variety of amines in DMF then afforded the corresponding urea derivatives **45**. Finally, cleavage from the resin and stereoselective cyclization afforded mimetics **46**, which were observed to be the major products by LC-MS and NMR analysis. Twelve compounds were synthesized in good yields and mimetics containing indole, phenol, imidazole, alcohol, and amino ester functionalities were produced (58% average yield over eight steps on support).

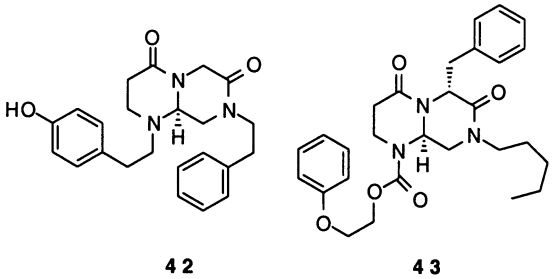

Figure 15. Analgesic compounds.

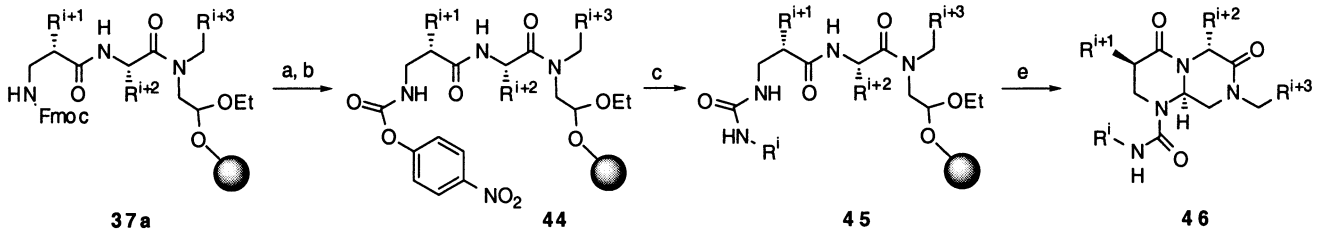

Scheme 4. (a) 20% Piperidine, DMF; (b) ClC(O)ONp, *i*-Pr_2NEt (5 equiv.); (c) primary amine (4 equiv.) in DMF; (d) formic acid, rt.

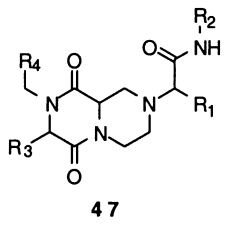

Figure 16. Bicyclic diketopiperazine scaffold.

The ability to access four points of diversity makes this scaffold a promising one, and the facility upon which the cyclization occurs should allow for the rapid synthesis of multiple derivatives in a parallel format. Good overall yields were observed for the compounds synthesized by either route. Furthermore, the scaffold draws upon a pool of readily accessible building blocks.

4.2. Bicyclic diketopiperazines

Golebiowski and co-workers have prepared two bicyclic diketopiperazine heterocycles utilizing independent synthetic sequences. The first report[36] is based on a Petasis reaction/cyclization sequence to provide mimetic **47** (Fig. 16).

The orthogonally protected piperazine-2-carboxylic acid core fragment **48** is first loaded onto hydroxymethyl-polystyrene resin via Mitsonobu reaction, and the Boc group removed under standard conditions to afford **49**. Petasis reaction cleanly provides immobilized carboxylic acid **50** with boronic acid inputs introducing diversity at the R^1 position. The R^2 input is subsequently introduced by standard amide bond formation to supply the resin-bound amide **51**. Deprotection of the α-nitrogen followed by standard *N*-Boc-α-amino acid coupling, deprotection and cyclative cleavage introduces the R^3 substituent and affords bicyclic product **47** (Scheme 5).

Using the Robbins Flex-Chem system, the authors constructed a library over the course of seven days. Although the number of compounds was not disclosed, the solid-phase Petasis reaction and cyclative cleavage strategy resulted in products with reasonably high purities (70–88%) by LC-MS analysis. Six representative examples were reported, suggesting that a considerable amount of structural diversity can be obtained (Fig. 17). Because racemic piperazine-2-carboxylic acid was employed, all four possible isomers were present in each final compound pool. The synthetic route allows for the control of three of the four chiral centers, with the Petasis reaction occurring in a stereorandom fashion. Overall, the rapid synthetic scheme and ready availability of three of the four starting materials makes this particular report a timely one.

One limitation of the aforementioned synthesis strategy is the absence of functionality at the $i+2$ position. In order to address the side chain omission, the authors communicated a second report which focuses upon the construction of a scaffold with five different sites of diversity, including the $i+2$ position (R^3 site in Fig. 18).[37] In addition, the second generation scaffold presents the R^3 backbone amide which more closely resembles the natural peptide backbone. The solid-phase synthesis is based on an Ugi/cyclative cleavage reaction sequence.

To initiate solid-phase synthesis, core fragment N^2-Boc-N^3-Fmoc-2,3-diaminopropionic acid was attached to hydroxymethyl polystyrene resin using Mitsonobu conditions to provide resin ester **60** (Scheme 6). Standard Fmoc deprotection exposed the amine which was used as the support-bound input for the Ugi reaction along with 2,6-dimethylphenylisonitrile and *R*-(+)-2-bromopropionic acid to afford α-bromo acid **61**. Deprotection and *i*-Pr_2NEt mediated S_N2 cyclization afforded monocyclic intermediate **62**. This intermediate was then elaborated to final product **63** by coupling with *N*-Boc-Phe-OH followed by TFA mediated Boc deprotection and cyclization in 2 M AcOH/*i*PrOH. The target compound was isolated in 20% yield (82%/step) and

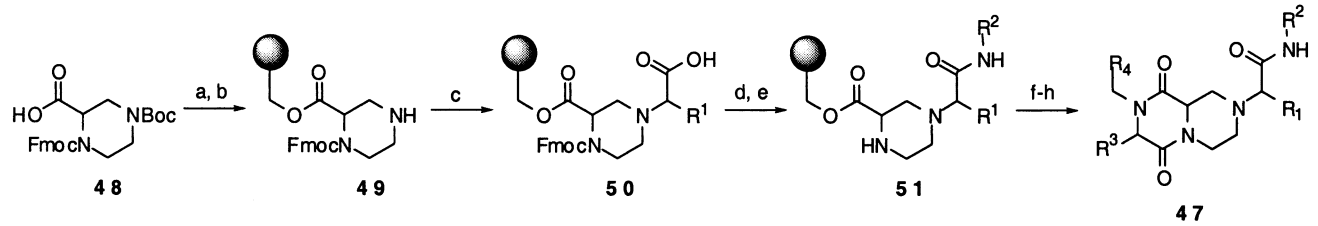

Scheme 5. (a) Hydroxymethylpolystyrene resin, Ph_3P, DEAD, THF; (b) 40% TFA/DCM, rt, 1 h; (c) $OHCCO_2H{\cdot}H_2O$, R-$B(OH)_2$, DCM; (d) 1,3-diisopropylcarbodiimide, primary amine, DCM; (e) 25% piperidine, DMF; (f) *N*-Boc-α-amino acid, benzotriazole-1-yl-oxy-tris-pyrrolidino-phosphonium hexafluorophosphate, DMF, rt; (g) TFA/DCM 25%, rt, 1 h; (h) 2 M AcOH, *i*-BuOH, 50°C, 24 h.

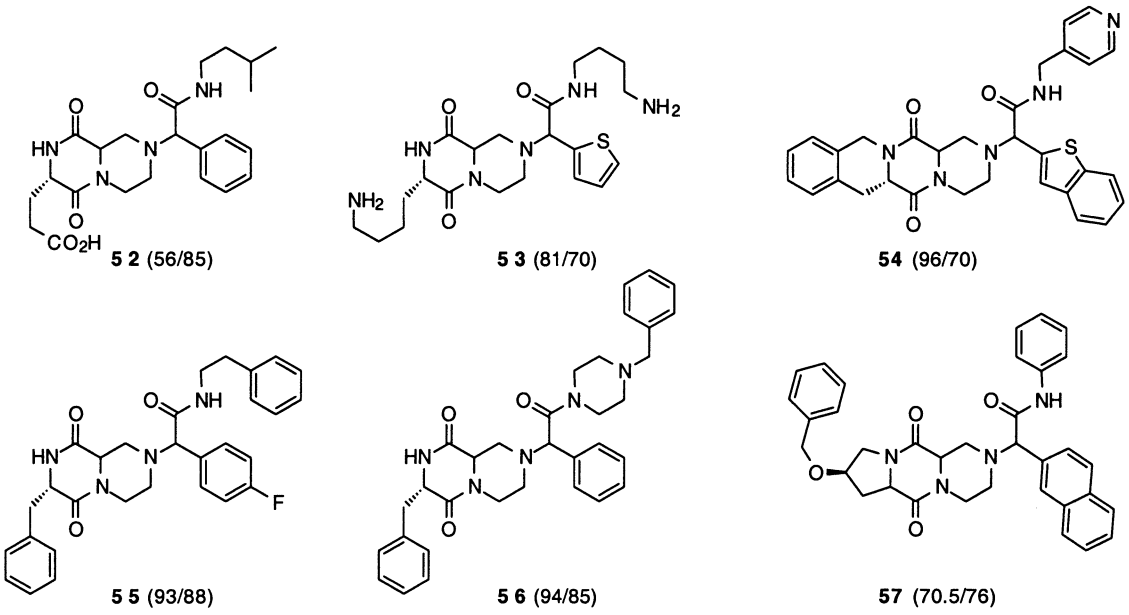

Figure 17. Representative examples with isolated yields and purities by LC-MS analysis.

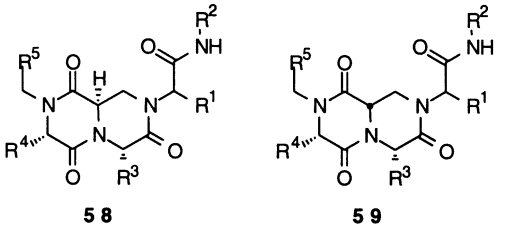

Figure 18. Second generation scaffold.

in good purity (85%) as determined by HPLC with UV detection.

This synthetic sequence has the potential to be quite versatile in that five potential sites of diversity are available, and the building blocks are either readily accessible or commercially available. Three of the four stereocenters can be controlled, with the Ugi reaction producing an approximate 1:1 mixture of isomers. Because a single compound was produced with hydrocarbon side chains, the scope and limitations of the chemistry has yet to be determined. However, this scaffold should allow for considerable application in the near future.

Kahn and Kim reported bicyclic diketopiperazine **70** that is constructed in seven steps from three backbone components in solution.[38] As depicted in Scheme 7, the synthesis is initiated by the acylation of *N*-benzyl-glycine ethyl ester, **64**, with *N*-Boc-Ala-OH to provide the tertiary amide **65** in quantitative yield. Ester hydrolysis and subsequent coupling with cyanomethylene–triphenylphosphorane furnished intermediate **66** in 71% yield. Following ozonolysis, the ensuing activated ketoacid was coupled to *N*-benzyl-Gly-OEt to afford the ketoamide **67** in 41% yield. TFA mediated *N*-Boc deprotection and cyclization lead to the formation of bicyclic adduct **69** through the intermediacy of tautomers **68**.

Final reduction of the olefin with hydrogen and platinum oxide afforded structure **70** in 43% overall yield for the final two steps. Although only one compound was synthesized, the use of *N*-substituted amino esters and Boc amino acids as the three backbone components could potentially allow for a significant amount of variability. The generality of the cyclization with respect to varying side chain stereochemistries and functionalities, however, has yet to be demonstrated. Overall, this contribution shows considerable promise as a solution phase alternative

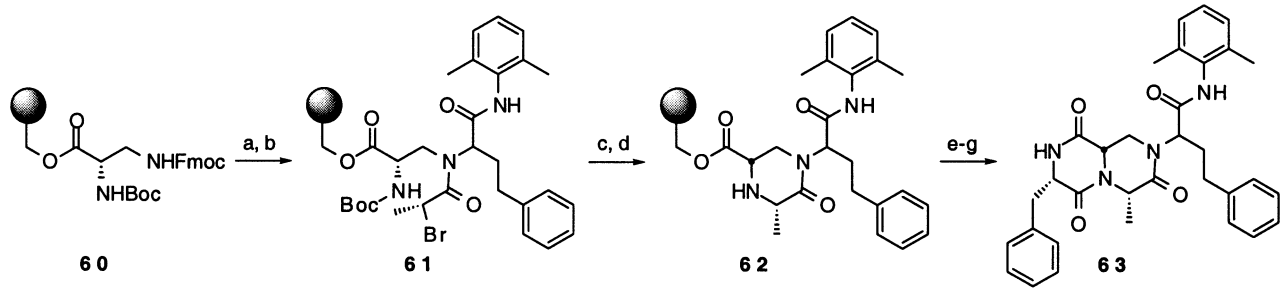

Scheme 6. (a) 25% Piperidine, DMF, 30 min; (b) hydrocinnamaldehyde (5 equiv.), 2,6-dimethylphenyl isonitrile (5 equiv.), *R*-(+)-2-bromopropionic acid, MeOH/$CHCl_3$ (1:4; v/v), rt 2×2 h; (c) 25% TFA, DCM; (d) 10% *i*-Pr_2NEt, DCM, rt, 18 h; (e) *N*-Boc-Phe-OH, NMM, isobutyl chloroformate, THF/DMF; (f) 25% TFA, DCM; (g) 2 M AcOH, *i*-PrOH, 50°C, 18 h.

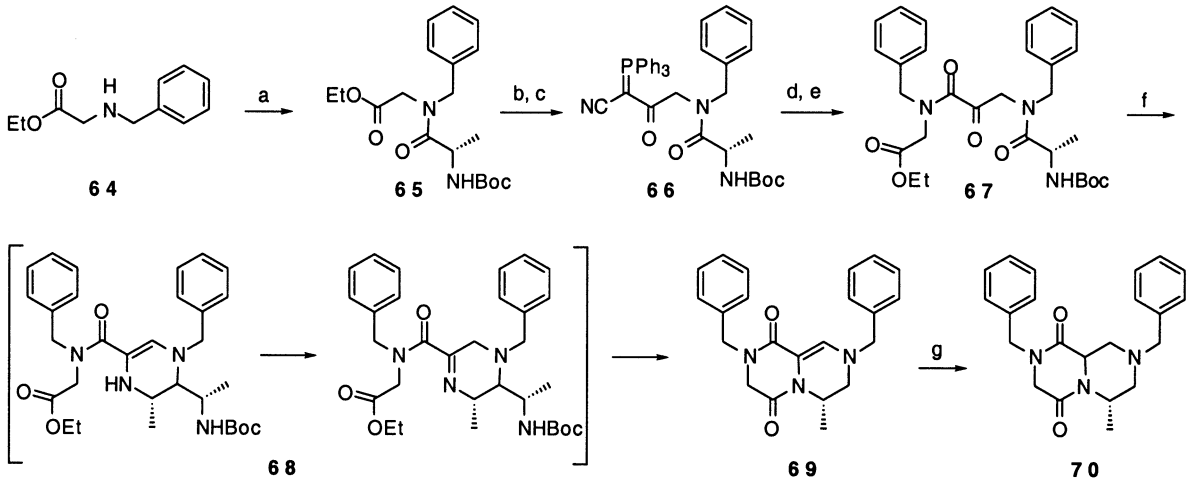

Scheme 7. (a) *N*-Boc-Ala-OH, 1-ethyl-3-(3′-dimethylaminopropyl)carbodiimide·HCl, 1-hydroxybenzotriazole, 100%; (b) LiOH, H_2O/THF, 100%; (c) $PH_3P{=}CHCN$, 1-ethyl-3-(3′-dimethylaminopropyl)carbodiimide·HCl, DMAP, CH_2Cl_2, 71%; (d) O_3, CH_2Cl_2, −78°C; (e) *N*-benzyl-Gly-OBn, 41%; (f) TFA, then workup with saturated $NaHCO_3$, 77%; (g) H_2, PtO_2, MeOH, 56%.

to Golebiowski's solid-phase bicyclic diketopiperazine mimetic synthesis.

5. Macrocyclic turn mimetics

5.1. S_NAr Cyclization

Burgess, Feng and co-workers reported an initial effort[39] towards the solid-phase synthesis of cyclic β-turn mimetics via S_NAr cyclization, and followed up with a detailed account of the optimized solid-phase sequence.[40] The authors noted their selection criteria for structure **72** (Scheme 8) is its potential to form a ring that would induce a β-turn in the peptidic fragment, in addition to the potential of the support-bound S_NAr as a facile method for preparing these compounds. The mimetic is composed of two variable amino acid residues and one constant residue which are all constrained by an aryl motif. Thus, the mimetic draws exclusively on the chiral pool for its diversity.

The key step in the preparation of these β-turn mimetics is the S_NAr mediated macrocyclization reaction of a support-bound nucleophile and a tethered fluorobenzene derivative (Scheme 8). Substrates **71** were formed on Tentagel S Ram resin (0.3 mmol/g) functionalized with the Rink linker. The amino acid side chains were protected as *tert*-butyl esters or *N*-Boc carbamates where appropriate, and the penultimate resin-bound intermediates were synthesized using conventional peptide synthesis. The products were cyclized under basic conditions, and then cleaved from the resin using

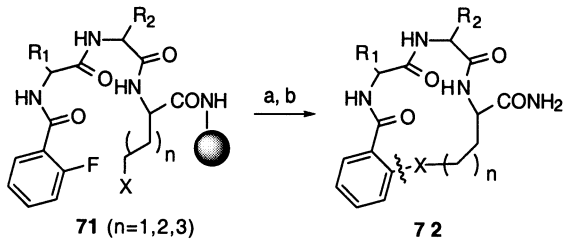

Scheme 8. (a) K_2CO_3, DMF, 30 h; (b) TFA.

acidic treatments. Rings of variable size were obtained using different nucleophilic heteroatoms introduced by amino acids displaying alcohol, thiol or amine containing side chains. For the 13- and 14-membered nitrogen-bound rings, the nucleophiles were generated via support-bound Hoffman degradation by the treatment of Asn and Gln with bis(trifluoroacetoxy)iodobenzene.

Thirteen compounds were synthesized and the yields were calculated by mass balance after preparative HPLC. Three 13-membered rings were constructed with oxygen and sulfur nucleophiles in 21–38% yield. Of the remaining entries, 14- to 16-membered rings were prepared with oxygen and nitrogen nucleophiles in variable yields (30–89%). With these initial studies in hand, the authors embarked on a detailed optimization effort to find the ideal conditions for the solid-phase preparation of turn mimetic libraries. The reaction conditions were optimized for the ideal resin types, resin loadings, bases, linker/spacers, and cyclization times.

In order to critically assess the efficacy of various possible nucleophilic side chains for the S_NAr mediated macrocyclization of differentially sized rings, thiol (Cys), alcohol (Ser, Homoser, and Thr), and amine (Orn, Lys, and Hoffman degradation products of Asn and Gln) containing residues were investigated. The use of various bases was explored simultaneously with the different nucleophiles, and it was found that a different base was optimal for each nucleophilic heteroatom. The use of cysteine derived nucleophiles lead to 13-membered products that were heavily contaminated with cyclic dimer byproducts. Amino acid spacers such as glycine led to increased levels of dimerized products, and larger ring sizes were not explored with the thiol linkage. While the oxygen nucleophiles were effective in the S_NAr cyclization of the 14-membered rings, the optimal bases (CsF and TBAF) led to significant racemization of the α-center of these residues in the final products. Nitrogen nucleophiles, however, cyclized cleanly to form 14- to 16-membered ring products. The optimal base was found to be K_2CO_3 in DMF, and no racemization was detected when these conditions were employed. The yields of the

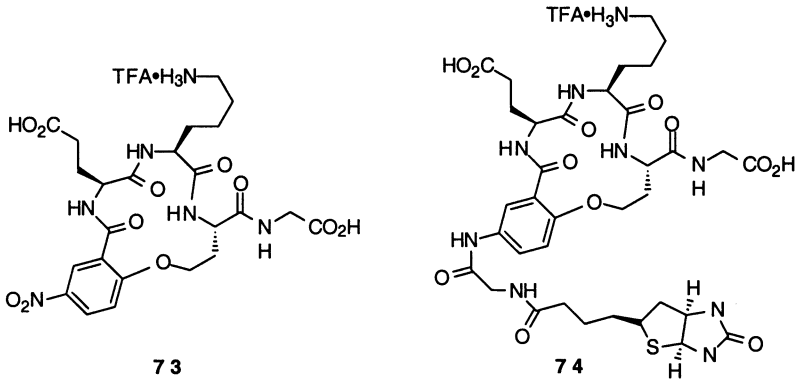

Figure 19. NGF mimetic and biotinylated derivative.

14- to 16-membered rings were moderate to good (23–89%), with the 13-membered rings forming in low yields (9%). Alcohol, amine, and alkyl side chains were present in the final products.

To assess the ability of turn mimetics **72** to serve as ligands for protein-protein interactions, a collection of compounds was evaluated for activation of tyrosine receptor kinase A, a cell surface receptor that binds nerve growth factor (NGF). In this study, the authors synthesized 60 turn mimetics with side chains based on the previously implicated turn portions of Trk C ligands NGF and mAb 5C3, although the number of compounds evaluated was not disclosed. Compound **73** was identified as an antagonist to TRK A (Fig. 19).[41] Facscan analysis of the binding of biotinylated derivative **74** to 4–3.6 cells (p75 Trk A+) showed a four-fold increase

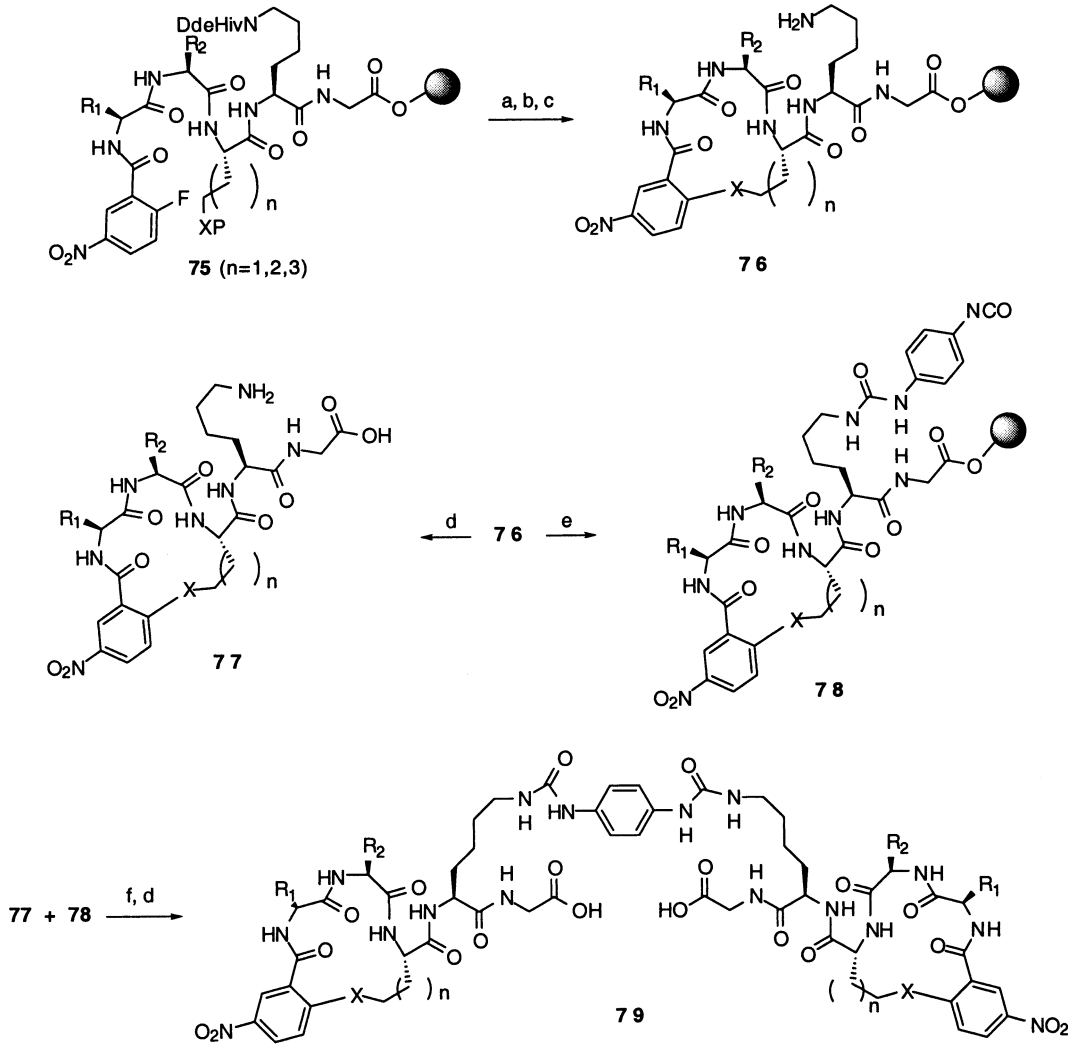

Scheme 9. (a) 1% TFA, 4% HSi*i*Pr$_3$, CH_2Cl_2; (b) K_2CO_3, DMF; (c) 2% N_2H_4, DMF; (d) TFA; (e) *i*Pr$_2$EtN, 1,4-diisocyanatobenzene; (f) *i*Pr$_2$EtN.

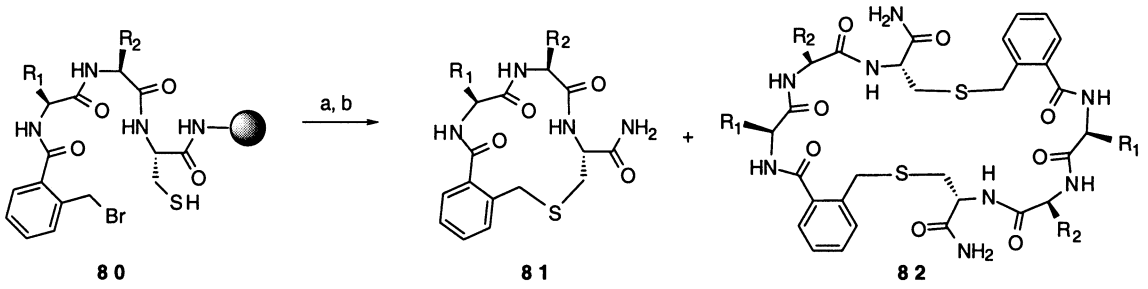

Scheme 10. (a) Base, DMF, 20 h; (b) TFA.

in fluorescence relative to a biotinylated control peptide. Furthermore, facscan analysis and ELISA assay demonstrated a dose dependant inhibition of mAb 5C3 binding to 4–3.6 cells with an IC_{50} value of 4 μM.

In addition, the ability of **73** to potentiate trophic effects was probed in cell based assays with dissociated primary neuronal cultures that are dependent on Trk A agonists for survival. This mimetic alone was found to have a protective effect on these cells, and the protection was enhanced in the presence of NGF. When acting alone, a 2 μM treatment of mimetic **73** was found to be comparable to 10 pM NGF. The authors also reported the compound to be resistant to papain and trypsin digestion.

In a second effort targeting mimetics of neurotrophin 3 (NT3), six monomeric turn mimetics and their corresponding dimeric derivatives were evaluated for their ability to stimulate cells that overexpress TrkC, the receptor for NT3.[42] This was performed by cytosensor microphysiometry. As displayed in Scheme 9, the monomers **76** were coupled together using a 'divergent–convergent' approach. Cyclization of **75** provided monomers **76** that were separated into two portions. One portion of each was cleaved and purified by preparative HPLC (**77**), while the other was elaborated into resin-bound isocyanate **78**. The cleaved monomers **77** were then coupled to the corresponding support-bound isocyanates, and the resultant dimers **79** cleaved from support and purified. Both the monomers and dimers were then evaluated for cell surface receptor binding and activation in a microphysiometry assay that measures the receptor activation mediated increase in extracellular acidification rates (ECARs). Two monomers gave a moderate response (5–10%), while three dimers were found to increase ECAR by 22–35% above the basal level. These three dimers contained amino acid sequences corresponding to Thr and Gly and/or Gly and Asp at the R^1 and R^2 positions, respectively, and all were 15-membered rings. The authors noted that other pharmacological data was necessary to confirm and quantitate the activities of these compounds.

5.2. S_N2 Cyclization

Burgess and coworkers described the synthesis of a second class of turn-like macrocycles[43] that were constructed via support-bound S_N2 macrocyclization (Scheme 10). Cyclization of benzyl bromide **80** was readily accomplished with base. All of the monomeric products **81** were heavily contaminated with the corresponding dimeric byproducts **82**. Thirteen compounds were prepared in 27% yield on average, with 13- to 16-membered rings being formed. The functional group display consisted primarily of alkyl and protected amine containing side chains, and the stereochemical display was limited to diastereomers of exclusively L-amino acids. Finally, dimer formation compromises the direct screening of libraries of macrocycles without rigorous purification.

6. Freidinger-type lactams

Piscopio and co-workers have developed two independent methodologies for the parallel synthesis of the Freidinger lactam class of external turn mimetics. The scaffold was designed to be a two-carbon homologue of the original Freidinger lactam, which was one of the first successful external turn mimetic scaffolds utilized.[9] Notably, the seven-membered lactam scaffold has also been employed as a mimetic of the γ-turn.[44]

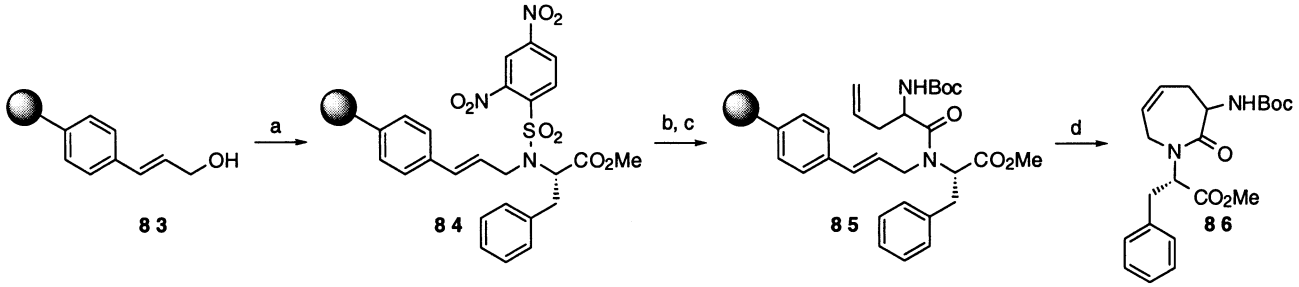

Scheme 11. (a) 2-(-2,4-Dinitro-benzenesulfonylamino)-3-phenyl-propionic acid methyl ester, DEAD, PPh_3, THF, rt, 16 h; (b) *i*-$BuNH_2$, CH_2Cl_2, rt, 2 h; (c) *N*-Boc-allylglycine, 1-methyl-2-chloropyridinium iodide, *i*-Pr_2NEt, CH_2Cl_2, reflux, 16 h; (d) $RuCl_2(=CHPh)(Pcy_3)_2$ (5 mol%), 1,2 dichloroethane, 80°C, 16 h, 16% from **83**.

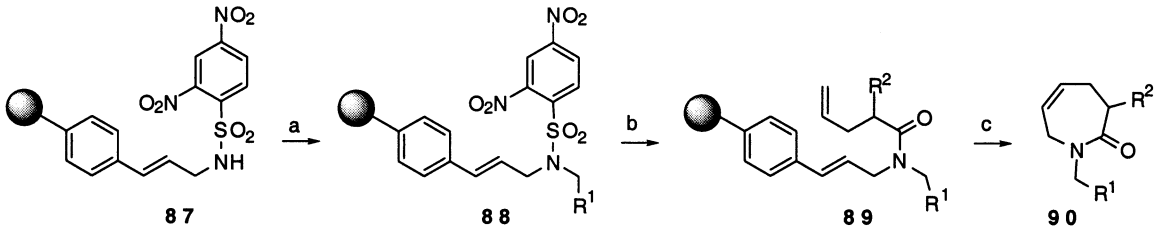

Scheme 12. (a) Alcohol, DEAD, PPh_3, THF, rt, 16 h, 69%; (b) *n*-$BuNH_2$, CH_2Cl_2, rt, 1 h; (c) δ-ω-unsaturated carboxylic acid, bromo-tris-pyrrolidino-phosphomium hexafluorophosphate, *i*-Pr_2NEt, DMF, 48 h or *O*-(7-azabenzotriazol-1-yl)-*N*,*N*,*N*′,*N*′-tetramethyluronium hexafluorophosphate, *i*-Pr_2NEt, DMF, rt, 16 h; (d) $RuCl_2(=CHPh)(Pcy_3)_2$ (5 mol%), 1,2 dichloroethane, 80°C, 16 h.

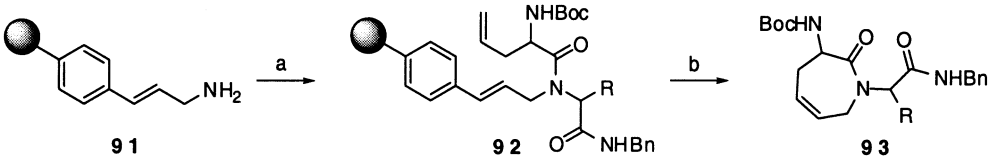

Scheme 13. (a) *N*-Boc-allylglycine, benzylisonitrile, aldehyde, MeOH, CH_2Cl_2, rt, 48 h; (b) $RuCl_2(=CHPh)(Pcy_3)_2$ (5 mol%), 1,2 dichloroethane, 80°C, 16 h.

6.1. First generation cyclative cleavage strategy

The key step in the solid-phase synthesis of mimetic **86** is the ring closing metathesis of a polymer supported α-ω-diene to afford the corresponding unsaturated seven-membered lactam (Scheme 11) with concomitant cleavage.[45] In order to determine whether the support-bound olefin could effectively serve as a traceless linker, the authors constructed the immobilized diene **85**. The 2,4-dinitrobenzenesulfonamide of phenylalanine methyl ester was first loaded onto Frechet's cinnamyl alcohol resin **83** using Mitsonobu conditions. The support-bound Fukuyama sulfonamide **84** was then cleaved with *n*-butyl-amine, and the resultant amine acylated with racemic *N*-Boc-allylglycine to afford the penultimate diene **85**. Treatment of the resin with a solution of Grubb's catalyst in 1,2 dichloroethane at 80°C for 6 h afforded the desired lactam **86** in 16% yield and in greater than 90% purity as a 1:1 mixture of diastereomers.

The authors next addressed the limitation of using the non-commercially available 2,4-dinitrobenzenesulfonamide protected amino esters as starting materials.[46] To this end, Frechet resin **83** was converted to the 2,4-dinitrosulfon-amide resin **87** (Scheme 12). Mitsonobu reaction with the desired alcohol then furnished intermediate **88**. The sulfon-amide was then cleaved with *n*-butylamine, and the resultant amine capped with the desired δ-ω-unsaturated pentenoic acid derivative to afford acyclic diene precursor **89**. The cyclization was carried out as before to afford the final products **90** in reasonable yields (average of 30% over four steps) and excellent purities (average of 95% by ^1H NMR), with ten compounds being reported. The collection of compounds includes side chains displaying primary alcohols in addition to a secondary alcohol and an α-hydroxy ester. In addition, both *N*-Boc-allylglycine and α-substituted δ-ω-unsaturated pentenoic acid derivatives were incorporated successfully. The synthetic sequence allows for three potential sites of diversity upon cyclization, while also providing possible sites for resin-bound manipulation.

6.2. Ugi/ring closing metathesis strategy

The authors reported a second complimentary approach to the Freidinger lactam[47] class of turn mimetics which utilizes a support-bound Ugi reaction to install three components of diversity. The Ugi inputs are the resin-bound allylic amine **91**, which is prepared from Frechet's cinnamyl resin **83**, *N*-Boc-allylglycine, an aldehyde and an isonitrile (Scheme 13). Following the Ugi reaction as depicted in Scheme 13, the immobilized resin-bound dienes **92** are washed and subjected to RCM catalysis to afford the desired lactams **93** as diastereomeric mixtures in moderate to good yields after two synthetic operations (Table 6).

As a final example, the synthesis of a four amino acid turn mimetic **96** was described (Scheme 14). Treatment of the cinnamyl amine resin **91** with a dipeptide acid, aldehyde, and isonitrile afforded the immobilized Ugi product **94**. This linear tripeptide was then subjected to Grubb's catalyst in 1,2 dichloroethane at 80°C to afford cyclic mimetic **95**, and subsequent TFA treatment produced the final product **96** in 61% yield and >95% purity after trituration in ether.

The two complimentary solid-phase sequences draw upon a pool of readily accessible alcohols, aldehydes, and iso-nitriles, while the use of substituted allylglycine and δ-ω-pentenoic acid derivatives is relegated to custom synthesis. The ease and speed in which the Freidinger-type lactams

Table 6. Freidinger lactams **93**

Entry	R	Yield (%)
1	*i*-Pr	62
2	$PhCH_2CH_2$	56
3	Ph	21

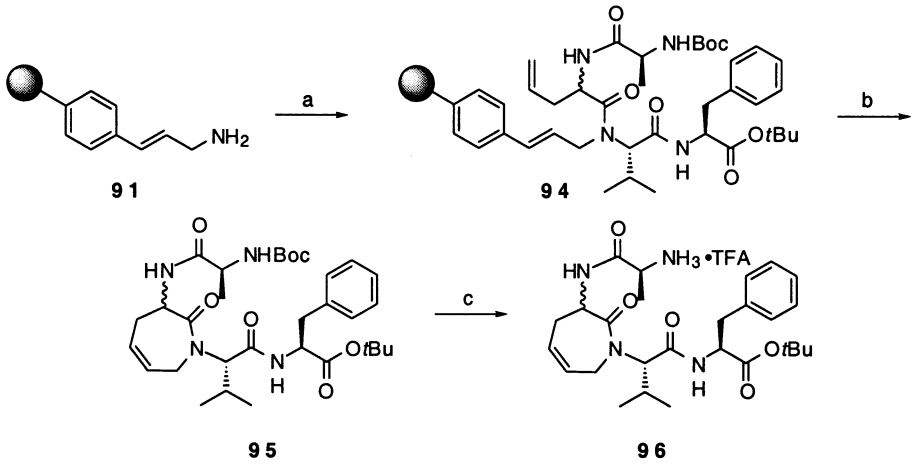

Scheme 14. (a) Isobutyraldehyde, *t*-butyl 2-isocyano-3-phenyl propionate, *N*-Boc-protected dipeptide, CH_2Cl_2, MeOH, rt, 48 h; (b) $RuCl_2(=CHPh)(Pcy_3)_2$ (5 mol%), 1,2 dichloroethane, 80°C, 16 h; (c) TFA, CH_2Cl_2, rt, 16 h, 55% overall.

can be accessed is unmatched. As a point of interest, these successful efforts represent the lone entry into combinatorial libraries of external turn mimetics.

7. Conclusions

The highly abundant β-turn motif has considerable importance in a large number of physiological interactions, and a significant amount of effort has been focused on the design and synthesis of small molecule turn mimetics. However, the design and synthesis of individual turn mimetics has generally not resulted in bioactive compounds due to the difficulty in both predicting and reproducing the display of side chains in the biologically active conformation of the corresponding peptide. For this reason, the application of combinatorial chemistry methods to the synthesis of libraries of β-turn mimetics has emerged as an active field, and several different reports on the parallel synthesis of turn mimetics have appeared since the original contribution in 1994.[16] These include both internal and external mimetics, with the former consisting of four distinct classes of heterocycles. In addition, the screening of several of these libraries towards biological targets has culminated in the identification of potent and subtype selective SRIF mimetics, $\alpha_4\beta_1$receptor antagonists, MCR1 agonists, NT3 and NGF mimetics, and opioid receptor agonists. Future endeavors will undoubtedly involve additional applications of the existing chemistry, as well as further advancement of methodologies to produce new libraries based upon the β-turn.

Acknowledgements

This work was generously supported by the National Institutes of Health (GM-53696). A. J. S. is grateful to the American Chemical Society, Organic Division (sponsored by Abbott Laboratories) for a generous fellowship. This manuscript is dedicated to the memory of Dr Timothy P. Kogan.

References

1. (a) Sawyer, T. K. In *Structure-Based Design: Diseases, Targets, Techniques and Developments*, Verrapandian, P., Ed.; Marcel Dekker: New York, 1997; pp. 559–634. (b) Freidinger, R. M. *TIPS Rev.* **1989**, *10*, 270. (c) Hirschmann, R. *Angew. Chem., Int. Ed. Engl.* **1991**, *30*, 1278. (d) Hirschmann, R.; Nicolau, K. C.; Pietranico, S.; Leahy, E. M.; Salvino, J.; Arison, B.; Cichy, M. A.; Spoors, P. G.; Shakespeare, W. C.; Sprengeler, P. A.; Hamley, P.; Smith III, A. B.; Reisine, T.; Raynor, P. A.; Maechler, L.; Donaldson, C.; Vale, W.; Freidinger, R. M.; Cascieri, M. R.; Strader, C. D. *J. Am. Chem. Soc.* **1993**, *115*, 12550. (e) Farmer, P. S. *Drug Design*; Ariens, E. J., Ed.; Academic: New York, 1980; Vol. 10, p. 119.
2. Gante, J. *Angew. Chem., Int. Ed. Engl.* **1994**, *33*, 1699.
3. Rose, G. D.; Gierasch, L. M.; Smith, J. A. *Adv. Protein Chem.* **1985**, *37*, 109.
4. (a) Kahn, M., Ed. *Tetrahedron* **1993**, *49*, Symposia 50, 3433. (b) Gillespie, P.; Cicariello, J.; Olson, G. H. *Biopolymers* **1997**, *43*, 191. (c) Fink, B. E.; Kym, P. R.; Katzenellenbogen, J. A. *J. Am. Chem. Soc.* **1998**, *120*, 4334. (d) Hirschmann, R.; Hynes, J.; Cichy-Knight, M. A.; van Rijn, R. D.; Sprengeler, P. A.; Spoors, P. G.; Shakespeare, W. C.; Pietranico-Cole, S.; Barbosa, J.; Liu, J.; Yao, W.; Rohrer, S.; Smith III, A. B. *J. Med. Chem.* **1998**, *41*, 1382.
5. Ball, J. B.; Alewood, P. F. *J. Mol. Recognit.* **1990**, *3*, 55.
6. For a review of dipeptide isosteres see: Hanessian, S.; McNaughton-Smith, G.; Lombart, H. G.; Lubell, W. D. *Tetrahedron* **1997**, *53*, 12789.
7. For a review of cyclic peptides see: Stradley, S. J.; Rizo, J.; Bruch, M. D.; Stroup, A. N.; Gierasch, L. M. *Biopolymers* **1990**, *29*, 263.
8. Olson, G. L.; Voss, M. E.; Hill, D. E.; Kahn, M.; Madison, V. S.; Cook, C. M. *J. Am. Chem. Soc.* **1990**, *112*, 323.
9. Freidinger, R. M.; Veber, D. F.; Perlow, D. S.; Brooks, J. R.; Saperstein, R. *Science* **1980**, *210*, 656.
10. Nagai, U.; Sato, K. *Tetrahedron Lett.* **1985**, *26*, 647.
11. Virgilio, A. A.; Ellman, J. A. *J. Am. Chem. Soc.* **1994**, *116*, 11580.
12. Souers, A. J.; Schürer, S.; Kwack, H.; Virgilio, A. A.; Ellman, J. A. *Synthesis-Stuttgart* **1999**, 583.

13. Maeji, N. J.; Valerio, R. M.; Bray, A. M.; Campbell, R. A.; Geyson, H. M. *React. Polym.* **1994**, *22*, 203.
14. Virgilio, A. A.; Bray, A. A.; Zhang, W.; Trinh, L.; Snyder, M.; Morrissey, M. M.; Ellman, J. A. *Tetrahedron* **1997**, *53*, 6635.
15. Virgilio, A. A.; Scürer, S. C.; Ellman, J. A. *Tetrahedron Lett.* **1996**, *37*, 6961.
16. Patel, Y. C. *J. Endocrinol. Invest.* **1997**, *20*, 348.
17. (a) Veber, D. F.; Saperstein, R.; Nutt, R. F.; Freidinger, R. M.; Brady, S. F.; Curley, P.; Perlow, D. S.; Paleveda, W. J.; Colton, C. D.; Zacchei, A. G.; Tocco, D. J.; Hoff, D. R.; Vandlen, R. L.; Gerich, J. E.; Hall, L.; Mandarino, L.; Cordes, E. H.; Anderson, P. S.; Hirschmann, R. *Life Sci.* **1984**, *34*, 1371. (b) Hocart, S. J.; Reddy, V.; Murphy, W. A.; Coy, D. H. *J. Med. Chem.*. **1995**, *38*, 1974.
18. (a) Veber, D. F.; Holly, F. W.; Paleveda, W. J.; Nutt, R. F.; Bergstrand, S. J.; Torchiana, M.; Glitzer, M. S.; Saperstein, R.; Hirschmann, R. *Proc. Natl. Acad. Sci. USA* **1978**, *75*, 2636. (b) Arison, B. H.; Hirschmann, R.; Paleveda, W. J.; Brady, S. F.; Veber, D. F. *Biochem. Biophys. Res. Commun.* **1981**, *100*, 1148. (c) Arison, B. H.; Hirschmann, R.; Veber, D. F. *Bioorg. Chem.* **1978**, *7*, 447.
19. (a) Pallai, P.; Struthers, S.; Goodman, M.; Rivier, J.; Vale, W. *Biopolymers* **1983**, *22*, 2523. (b) Murphy, W. A.; Heiman, M. L.; Lance, V. A.; Mezo, I.; Coy, D. H. *Biochem. Biophys. Res. Commun.* **1985**, *132*, 922.
20. Muskal, S. Unpublished Results. MDL Information Systems, Inc., San Leandro, CA.
21. Souers, A. J.; Virgilio, A. A.; Rosenquist, Å.; Fenuik, W.; Ellman, J. A. *J. Am. Chem. Soc.* **1999**, *121*, 1817.
22. For the synthesis of the five-membered amino acids: (a) Murray, P. J.; Starkey, I. D.; Davies, J. E. *Tetrahedron Lett.* **1998**, *39*, 6271. For the synthesis of the six-membered amino acid: (b) Souers, A. J.; Ellman, J. A. *J. Org. Chem.* **2000**, *65*, 1222.
23. Souers, A. J.; Rosenquist, Å.; Jarvie, E. M.; Ladlow, M.; Feniuk, W.; Ellman, J. A. *Bioorg. Med. Chem. Lett.* **2000**, *10*, 2731.
24. Virgilio, A. A. PhD Dissertation, University of California, Berkeley, CA, 1996.
25. Curley, G. P.; Blum, H.; Humphries, M. J. *Cellular Mol. Life Sci.* **1999**, *56*, 427.
26. Souers, A. J.; Virgilio, A. A.; Schürer, S.; Ellman, J. A.; Kogan, T. P.; West, H. E.; Ankener, W.; Vanderslice, P. *Bioorg. Med. Chem. Lett.* **1998**, *8*, 2297.
27. Cone, R. D. *Trends Endocrinol. Metabol.* **1999**, *10*, 211.
28. Chen, W. B.; Shields, T. S.; Stork, P. J. S.; Cone, R. D. *Anal. Biochem.* **1995**, *226*, 349.
29. Haskell-Luevano, C.; Rosenquist, Å.; Souers, A. J.; Khong, K. C.; Ellman, J. A.; Cone, R. D. *J. Med. Chem.* **1999**, *42*, 4380.
30. Kurokawa, K.; Kumihara, H.; Kondo, H. *Bioorg. Med. Chem. Lett.* **2000**, *10*, 1827.
31. Eguchi, M.; Lee, M. S.; Nakanishi, H.; Stasiak, M.; Lovell, S.; Kahn, M. *J. Am. Chem. Soc.* **1999**, *121*, 12204.
32. Vojkovsky, T.; Weichsel, A.; Patek, M. *J. Org. Chem.* **1998**, *63*, 3162.
33. Kahn, M.; Eguchi, M.; Kim, H.-O. US Patent 6,013,458, January 11, 2000.
34. Stasiak, M.; Eguchi, M.; Mehlin, C.; Kahn, M. *Pept. New Millennium*, Proc. Am. Pept. Symp. 16th **2000**, p. 233.
35. Eguchi, M.; Lee, M. S.; Stasiak, M.; Kahn, M. *Tetrahedron Lett.* **2001**, *42*, 1237.
36. Golebiowski, A.; Klopfenstein, S. R.; Chen, J. J.; Shao, X. *Tetrahedron Lett.* **2000**, *41*, 4841.
37. Golebiowski, A.; Klopfenstein, S. R.; Shao, X.; Chen, J. J.; Colson, A.; Grieb, A. L.; Russell, A. F. *Org. Lett.* **2000**, *2*, 2615.
38. Kim, H.; Nakanishi, H.; Lee, M. S.; Kahn, M. *Org. Lett.* **2000**, *2*, 301.
39. Feng, Y.; Wang, Z.; Jin, S.; Burgess, K. *J. Am. Chem. Soc.* **1998**, *120*, 10768.
40. Feng, Y.; Burgess, K. *Chem. Eur. J* **1999**, *5*, 3261.
41. Miliartchouk, S.; Feng, Y.; Ivanisevic, L.; Debeir, T.; Cuello, A. C.; Burgess, K.; Saragovi, H. U. *Mol. Pharm.* **2000**, *57*, 385.
42. Zhang, A. J.; Khare, S.; Gokulan, K.; Linthicum, D. S.; Burgess, K. *Bioorg. Med. Chem. Lett.* **2001**, *11*, 207.
43. Feng, Y.; Pattarawarapan, M.; Wang, Z.; Burgess, K. *Org. Lett.* **1999**, *1*, 121.
44. Brickmann, K.; Somfai, P.; Kihlberg, J. *Tetrahedron Lett.* **1997**, *38*, 3651.
45. Piscopio, A. D.; Miller, J. F.; Koch, K. *Tetrahedron Lett.* **1997**, *55*, 8189.
46. Piscopio, A. D.; Miller, J. F.; Koch, K. *Tetrahedron Lett.* **1998**, *39*, 2667.
47. Piscopio, A. D.; Miller, J. F.; Koch, K. *Tetrahedron* **1999**, *55*, 8189.

Biographical sketch

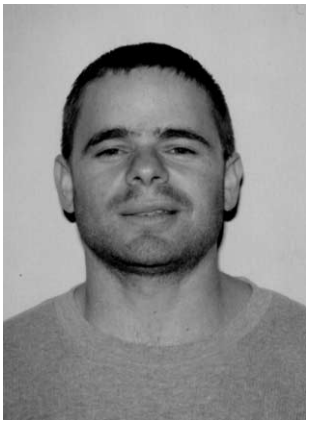

Andrew Souers received his B.S. degree from University of Wisconsin at Madison where he worked in the laboratories of Laura Kiessling. He recently earned his PhD degree working with Jonathan Ellman at University of California at Berkeley. His thesis research focused on the design, synthesis and evaluation of libraries of β-turn mimetics and on the development of novel sulfinyl-based ligands for asymmetric catalysis. While at Berkeley Andrew was awarded an American Chemical Society Division of Organic Chemistry Fellowship, a Pharmacia Graduate Fellowship, and the Department of Chemistry Bruce Mahan Award for teaching excellence. Currently, Andrew is a research scientist at Abbott Laboratories.

Jonathan Ellman received his B.S. degree from M.I.T. in 1984 where he worked in the laboratory of K. B. Sharpless. He completed his PhD degree with David A. Evans at Harvard University in 1989. After a NSF postdoctoral fellowship at the University of California at Berkeley with Peter G. Schultz, he joined the faculty at the University of California at Berkeley in 1992 where he is currently Professor of Chemistry. He holds a joint appointment at University of California at San Francisco in the Department of Cellular and Molecular Pharmacology. His laboratory is currently engaged in the development of new design strategies for the preparation of small molecule libraries, and in the application of small molecule libraries to different research problems in chemistry and biology. In addition, his group places a major emphasis on the development of practical and general synthesis methods that are applicable to both library synthesis and more traditional synthesis efforts.